RESEARCH ARTICLE

RUNNING HEAD: Acute hypoxia degraded protein in 24-day-old murine muscle

Six-hour hypoxia induced protein degradation in *M. gastrocnemius* of 24-day-old mice by activating FOXO1 and suppressing AKT-mTORC1

Jingyi Song,[1] Marcel Jaklofsky,[1] Claudia Carmone,[1] Vincent de Boer,[1] Niels Wever,[2] Jaap Keijer,[1] Sander Grefte [1]

[1] Human and Animal Physiology, Wageningen University, Wageningen, The Netherlands.
[2] Animal Nutrition, Wageningen University, Wageningen, The Netherlands.
Correspondence: *Sander Grefte (sander.grefte@wur.nl) and Jaap Keijer (jaap.keijer@wur.nl).*

ABSTRACT

Long-term hypoxia has been associated with skeletal muscle atrophy, including increased protein degradation over protein synthesis. This contrasts sharply with muscle hypertrophy and net protein synthesis occurring in developing skeletal muscle of young mice. Here, we aimed to understand the impact of acute, physiologically plausible environmental hypoxia on muscle proteostasis of the *M. gastrocnemius* of young mice. Fasted prepubertal, 24-day-old male B6JRccHsd(B6J)-*Nnt*$^{+}$/Wuhap mice with similar body weight and lean mass were exposed to normobaric hypoxia (12% O_2) or normoxia (20.9% O_2) for 6 hours. The transcriptome (n=12) and protein (n=6) responses of the *M. gastrocnemius* were analyzed. A hypoxic response of *M. gastrocnemius* was confirmed by increased expression of HIF1 (*Ankrd37* and *Ddit4*) and forkhead box-O (FOXO) 1 (*Depp1* and *Ddit4*) target genes. RNA-Seq analysis revealed that hypoxia activated FOXO signaling, which was confirmed by increased FOXO1 protein levels and decreased p-AKT/AKT ratio. Detailed mapping of the FOXO1 pathway suggests a strong FOXO1-mediated hypoxic effect on protein degradation and synthesis. A central role of *Atf4* is suggested by the hypoxic-dependent positive correlations with FOXO1, FBXO32, *Depp1, Eif4ebp1,* and *Ddit4*. Further analyses showed increased FBXO32, which positively correlated with FOXO1, and decreased p-S6K/S6K and p-4E-BP1/4E-BP1 ratios. Our results showed for the first time that a 6-hour exposure to 12% O_2 normobaric hypoxia in 24-day-old mice activates FOXO1 signaling in *M. gastrocnemius*, resulting in decreased protein synthesis and increased protein degradation most likely via reduced energy availability, which may be relevant for infant air or high altitude traveling.

NEW & NOTEWORTHY

We newly investigated an acute (6 hours) hypoxic exposure (12% O_2) in developing and growing *M. gastrocnemius* of 24-day-old mice. This acute hypoxia significantly enhanced muscle protein breakdown via the activation of FOXO1 and subsequently FBXO32, while also suppressing protein synthesis via the reduced p-S6K/S6K and p-4E-BP1/4E-BP1 and thus AKT-mTORC1 pathway. Together these changes observed could potentially hamper muscle development of young mice.

Keywords: Hypoxia, Skeletal muscle, Proteostasis, mTORC1, FOXO1

INTRODUCTION

In mammalian life, oxygen plays a crucial role in cellular energy production, for which over 90% of the cellular oxygen is used (1). As the largest tissue in the body, skeletal muscle contributes to approximately 21% of oxygen consumption (2) and 30% energy expenditure (3) in rest. Protein synthesis is one of the most energy consuming cellular processes (4), and decreased cellular energy reduces protein synthesis. Therefore, it is not surprising that reduced tissue oxygen availability (hypoxia), influences skeletal muscle metabolism, muscle mass and muscle function.

Long-term hypoxia, induced by high altitude or pulmonary diseases, leads to reduced muscle mass and myofiber cross-sectional area (CSA) in mice and humans (5, 6). Three-week normobaric hypoxia (8% O_2) induced profound muscle weight loss, decreased CSA and fiber-type transient toward the oxidative type I fibers in 1, 3 and 13 months old mice (5). In humans, 3-week hypoxia aggravated the loss of muscle mass during bed resting by decreasing CSA of both thigh and calf muscle (6). These results altogether suggest that hypoxia reduces muscle mass most likely due to higher muscle protein degradation over protein synthesis ratio. Mammalian target of rapamycin complex 1 (mTORC1) (7) and forkhead Box-O 1 (FOXO1) (8) are important in regulating skeletal muscle protein degradation and synthesis cumulatively known as muscle proteostasis. MTORC1 promotes protein synthesis by phosphorylating ribosomal protein S6 kinases (S6K) and translation initiation factor 4E-binding protein 1 (4E-BP1) (9). FOXO1 can induce protein degradation via the autophagy lysosomal pathway (ALP) and the ubiquitin-proteasome system (UPS) (10). UPS is responsible for the degradation of major muscle contractile proteins (11). During muscle atrophy, this pathway is activated by FOXO1 that increases gene expression of E3 ubiquitin ligases F-box protein 32 (FBXO32, Atrogin-1) and tripartite motif containing 63 (TRIM63, MuRF1). This process directs the polyubiquitination of proteins to target them for proteolysis by the 26S proteasome (12). Both mTORC1 and FOXO1 activity are regulated by serine-threonine protein kinase (AKT), with AKT activating mTORC1 and inhibiting FOXO1 signaling (9). MTORC1 and FOXO1 are also affected by long-term hypoxia. For example, 4-week hypoxia (11% O_2) decreased mTORC1 activity in the mouse liver (13), and 4-week hypoxia (12.4% O_2) stimulated FOXO1 signaling in the rats *extensor digitorum longus* (EDL) muscle (10).

Interestingly, a short hypoxia exposure has been shown to reduce AKT phosphorylation (2 hours, 8% O_2) (14) and increased FOXO1 signaling (6 hours, 12% O_2) (15) suggesting an acute response of FOXO1 signaling to hypoxic challenges. However, whether such acute exposure affects muscle proteostasis remains to be investigated. Therefore, this study aims to investigate the *in vivo* impact of acute 6-hour hypoxia (12% O_2) on cellular process focused on muscle proteostasis, including mTORC1 and FOXO1 signaling, in the *M. gastrocnemius* of prepubertal, 24-day-old mice. Current studies on the hypoxic response primarily focus on adult mice with a stable body weight. For this study, young prepubertal mice were investigated since their skeletal muscle undergoes rapid growth until adulthood, contributing to half of the gained body weight (16). This is primarily characterized by hypertrophy of myofibers with increasing CSA (17, 18), which in murine *M.* EDL and *M. soleus* were shown to nearly triple from day 21 to 42 (19). Skeletal muscle hypertrophy is primarily driven by higher protein synthesis exceeding protein degradation, mediated by the AKT-mTORC1 pathway (20). This contrasts with the stable muscle mass

observed in adult mice (21). It remains unknow whether and how proteostasis—the balance between protein synthesis and protein degradation—of growing skeletal muscle is influenced by acute hypoxia. Therefore, in this study the effect of acute (6-hour) hypoxia (12% O_2) was investigated for the first time in skeletal muscle of prepubertal, 24-day-old mice.

MATERIALS AND METHODS

Animals

Twenty-four male B6JRccHsd(B6J)-*Nnt*$^{+}$/Wuhap mice were obtained from an in-house breeding colony. Mice were housed under environmentally controlled conditions (23 ± 1 °C, 12 h/12 h light-dark cycle, 50 ± 10% humidity, chow diet). Mice were weaned at 21 days of age and were then individually housed with *ad libitum* access to chow diet and water. Body weight and lean mass were measured by EchoMRI Whole Body Composition Analyser (EchoMRI, US). Mice were randomly allocated based on lean mass to the experimental hypoxia (Hypox) group or the control normoxia (Norm) group (n = 12 per group). At 6 hours prior to light phase at day 24, all food was removed to ensure a fasted state at the start of the hypoxic exposure. At the beginning of light phase, oxygen concentration was decreased in 30 min from 20.9% to 12% (12% O_2 / 88% N_2; SOL, NL) in all cages of the Hypox group in 30 min using an air flow of 1 L/min. Then the air flow switched back to 0.430 L/min and was maintained for 6 hours. Mice in the Norm group were treated in the same manner but remained under normoxic conditions (ambient air; 20.9% O_2). Normobaric air pressure is standard in all situations. During the 6-hour exposure, physical activity was measured by breaks in infra-red beams at 5 mm distance from each other (TSE, DE). After the exposure, mice were immediately killed by decapitation. Blood glucose concentration was measured in whole blood using a Freestyle blood glucose system (Abbott Diabetes Care, NL) according to the manufacturer's instructions. *M. gastrocnemius* was excised, snap frozen in liquid nitrogen and stored at -80 °C until analyses. The experimental protocol for animal handling was in accordance with the EU Directive 2010/63/EU for animal experimentation and approved by the Animal Welfare Committee of Wageningen University, Wageningen, The Netherlands (2020.W-0019.003).

RNA isolation and RNA-Seq data analysis

The whole *M. gastrocnemius* was ground and 20 mg was further homogenized using the TissueLyser LT (Qiagen) for 6 min at 50 Hz after which total RNA was isolated with the TRIzol Reagent following the manufacturer's instructions (Thermo Fisher Scientific, US). RNA concentration and integrity were measured by Nanodrop One (Thermo Fisher Scientific, US) and Agilent 2200 TapeStation (Agilent Technologies Inc., USA. All samples met the criteria of a 260/280 and 260/230 ratio higher than 1.8 and a RNA integrity number (RIN) above 8 (n = 12 per group).

For whole genome transcriptome analysis of *M. gastrocnemius*, RNA preparation, library construction, sequencing on the Illumina platform (NovaSeq 6000 platform) and raw data filtering were performed by Novogene (CN). In short, mRNA was purified from total RNA using poly-T oligo-attached magnetic beads. After fragmentation, the first strand cDNA was synthesized using random hexamer primers, followed by the second strand cDNA synthesis using dUTP for a directional library. The directional library was completed by end repair, A-tailing, adapter ligation, size selection, USER enzyme digestion, amplification, and purification (In-house kit: Novogene NGS Stranded RNA Library Prep Set (PT044)). The library was checked with Qubit, real-time PCR for quantification, and bioanalyzer for size distribution detection. Quantified libraries were pooled and sequenced on NovaSeq 6000 platform using S4 flow

cells, according to effective library concentration and data amount. Raw data (raw reads) of FASTQ format were processed through in-house perl scripts to obtain clean data (clean reads) by removing reads containing adapter, reads containing ploy-N and low quality reads from raw data. Quality check of the clean reads was preformed using FASTQC (22). Clean reads were aligned to the mouse genome (Mus_musculus.GRCm39.108) using STAR2.7 (23), and counts were quantified using HTSeq (24). Average sequencing depth was 27M paired end reads, of which at least 86.6% were uniquely mapped. After counting, data analysis and statistical testing was performed in R 4.2.1 with DESeq2 (25).

RNA-Seq data analysis was based on a two-group comparison: Hypox mice (n = 12) versus Norm mice (n = 12) and all data were deposited in Gene Expression Omnibus (GEO) with accession ID: GSE255522. Related plots and heatmaps were generated use R packages according to Bekebrede *et al*. (26). Specifically, genes with total less than 10 counts in all samples were removed. Genes with adjusted P-value < 0.05 with Benjamini-Hochberg correction and absolute fold change > 0.07 were identified as differentially expressed genes (DEGs) and used to identify molecular and cellular pathways being affected.

Quantitative reverse transcription polymerase chain reaction (Q-PCR)

cDNA synthesis and real-time Q-PCR were performed. In brief, 1 µg total RNA was used for conversion to cDNA with the iScript cDNA synthesis kit (BioRad, US) in a final volume of 20 µL. Then 100x diluted cDNA was used for Q-PCR with 12.5 µL iQ SYBR Green Supermix (BioRad, US), 2 µL diluted cDNA, 1 µL forward primer (10 µM) and 1 µL reverse primer (10 µM) in a final volume of 25 µL. DEPP1 autophagy regulator (*Depp1*), DNA-damage-inducible transcript 4 (*Ddit4*) and ankyrin repeat domain 37 (*Ankrd37*) were target genes. Beta-2 microglobulin (*B2m*), calnexin (*Canx*), and hypoxanthine phosphoribosyltransferase (*Hprt1*) were used as reference genes. Primers were designed by NCBI Primer BLAST (27). Sequences and product lengths of target and reference genes can be found in Table S1. Data were expressed as relative gene expression based on reference genes (n = 12 per group).

Western blot

Six samples per group were randomly chosen for Western blot. Protein extraction of *M. gastrocnemius* was done by adding 300 µL of ice-cold lysis buffer (50 mM Tris-HCl, pH 7.4, 0.2% Triton X-100, 150 mM NaCl, 1 mM EDTA, NAM, 1 µM TSA, 20 mM NAM, protease inhibitor cocktail (Roche, AT) and phosphatase inhibitor tablet (Roche, AT)) to 15 mg frozen ground muscle tissue and lysed using Qiagen TissueLyser LT for 3 min at 50 Hz. Lysates were centrifuged for 5 min at 10 000 *g* at 4°C and supernatant was collected to determine protein concentration using Pierce BCA protein assay kit (Thermo Scientific, US). Fifteen µg protein was loaded per lane on NuPAGE 4%–12% BIS-TRIS gels (Invitrogen) and run according to manufacturer's instruction. Proteins were then transferred to Immobilon-FL PVDF membrane (Millipore, US). Membranes were stained with Revert 700 Total Protein Stain (LI-COR, DE) for total protein loading quantification and then destained. After blocking in 3% BSA in TBS at room temperature for 1 hour, membranes were incubated overnight with primary antibodies in 50% Intercept blocking buffer (LI-COR, DE) in TBS+0.1% Tween 20 at 4°C. Primary antibodies used were anti-AKT (1:1000; #9272S, Cell Signaling, NL), anti-p-AKT (S473) (1:500; #9271S, Cell Signaling, NL), anti-FOXO1 (1:1000; #ab52857, Abcam, UK), anti-FBXO32 (1:1000; #sc-166806, Santa Cruz, US), anti-TRIM63 (1:1000; #ab183094, Abcam, UK), anti-ubiquitin (1:500; #sc-8017, Santa Cruz, US), anti-DDIT4 (1:5000; #10638-1-AP, Proteintech), anti-4E-BP1 (1:500; #9644S, Cell Signaling, NL), anti-p-4E-BP1 (T37/46) (1:500; #2855, Cell Signaling, NL), anti-S6K (1:1000; #9202S, Cell Signaling, NL), anti-p-S6K (T389) (1:500;

#ab60948, Abcam, UK), anti-mTOR (1:1000; #2983, Cell Signaling, NL), and anti-p-mTOR (S2448) (1:1000; #5536, Cell Signaling, NL). Matched IR-dye-based secondary antibodies (LI-COR, DE) were used to detect antibody signals as follows: IRDye 800CW anti-Rabbit IgG (1:5000; #926-32213), IRDye 680RD anti-Mouse IgG (1:5000; #926-68072), and IRDye 800CW anti-Mouse IgG (1:5000; #926-32212). Membranes were scanned using an Odyssey scanner (LI-COR, DE). Total protein loading and target protein expression was quantified using Fiji ImageJ (28). Total protein loading was used for normalization of the target protein expression. Results between membranes were normalized based on mean expression of the Norm group.

Amino acid measurement

Amino acids in plasma were analyzed by ultra-performance liquid chromatography tandem mass spectrometry (UHPLC-MS/MS) using precolumn derivatization with 6-aminoquinolyl-N-hydroxysuccinimidyl carbamate (AccQTag Ultra) (29). For sample workup, 40 µL of acidified methanol (MeOH - 0.1% methanoic acid) was added to 10 µL of plasma samples and vortexed vigorously, followed by centrifugation for 10 min at 10 000 *g*. Twenty-five µL of supernatant was combined with 10 µL of internal standard mixture consisting of the canonical amino acid mix, Cambridge isotope laboratory MSK-CAA-1; L-Asparagine-13C4, 15N2 hydrate (LGC standards), L-glutamine-13C5 (LGC standards), L-cysteine-13C3 (LGC standards), in glass vials followed by evaporation to dryness at 60 °C under a gentle stream of nitrogen. The pellet was reconstituted in borate buffer (0.2M, pH 8.5), vortexed, and 20 µL AccQTag was added to each vial, mixed, and incubated at room temperature for 15 min, followed by incubation at 55 °C for 15 min. Finally, 900 µL of MQ was added.

The processed samples were injected (5 µL) on a Accucore PFP column (2.6 µm, 2.1 mm x 100 m) with matching guard column (Thermo Scientific) using a mobile phase linear gradient of 0.1% formic acid in MQ to 0.1% formic acid in acetonitrile on an Acquity UHPLC (Waters) at 0.4 mL/min. Detection of column elution was done on Quattro Premier XE triple-quadrupole (Waters) in positive ion mode using multiple reaction monitoring (n = 12 per group).

Statistics

The data were expressed as mean ± SD, geometric mean ± geometric SD for lognormal distribution data, and median (IQR) for non-normal data. Statistical analyses were performed using GraphPad Prism version 9.3.1 (Graphpad, USA), except for RNA-Seq data (see above). Data were checked for normality using the D'Agostino normality test. All normal data and lognormal data were analyzed by independent Student's unpaired t-tests, except for amino acid measurement where Welch t-test was used. Non-normal data were analyzed with a Mann-Whitney test. P-values < 0.05 were considered statistically significant.

RESULTS

Six-hour hypoxia activated FOXO1 signaling pathway in *M. gastrocnemius*

Prior to the hypoxia (12% O_2) exposure, mice with similar body weight (Figure 1A) and lean mass (Figure 1B) were assigned to the Hypox group or the Norm group. Physical activity was not changed during hypoxia (Figure S1). After 6 hours hypoxia exposure, blood glucose levels were not changed (Figure 1C). Based on our previous study (15, 30), target genes of hypoxia-inducible factor 1 (HIF1; *Ankrd37* and *Ddit4*) and FOXO1 (*Ddit4* and *Depp1*) were selected as hypoxia markers in the *M. gastrocnemius* tissue. Q-PCR analysis showed these genes were all upregulated in Hypox group (Figure 1D), which confirms the

hypoxic effect on the *M. gastrocnemius* and suggests the activation of HIF1 and FOXO1. In addition, only *Ddit4* was strongly positive correlated with *Depp1* in both Norm and Hypox groups (Norm: r = 0.958, P-value < 0.0001; Hypox: r = 0.927, P-value < 0.0001) (Figure 1E). The correlations of *Anrkd37* with *Depp1* (Norm: r = 0.185, P-value= 0.034; Hypox: r = -0.050, P-value = 0.002) and *Ddit4* (Norm: r = 0.129, P-value = 0.017; Hypox: r = -0.156, P-value = 0.024) were less strong and different in Norm and Hypox group. These results indicate a dominant role of FOXO1 in activating *Ddit4* and *Depp1*.

Transcriptome analysis of *M. gastrocnemius* was applied to gain molecular insight in the effect of 6-hour hypoxia (12% O_2) on skeletal muscle. To visualize variations between samples, 3D PCA analysis was performed with RNA-Seq Log transformed data (Figure 2A). A clear separation could be observed between Hypox (green) and Norm (blue) group, where principal component (PC) 1, PC2, and PC3 explained 23.67%, 14.92%, and 12.38% of the variation in the data, respectively. In total, 15508 genes with an unique Entrez annotation were detected in RNA-Seq, of which 2404 genes were differentially-expressed genes (DEGs, adjusted P-value < 0.05). 1333 DEGs were significantly upregulated (Log2 fold change (Log2FC) > 0), and 1071 DEGs were significantly downregulated (Log2FC < 0) in the Hypox group (Figure 2B). Consistent with the Q-PCR results, *Depp1*, *Ddit4* and *Ankrd37* were also upregulated in RNA-Seq, highlighted in the volcano plot (Figure 1D and 2B). *Foxo1*, activating *Depp1* and *Ddit4*, was upregulated in Hypox group (Figure 2B) and positively correlated with *Depp1* and *Ddit4* expression in Hypox group (Pearson r = 0.841, P-value = 0.001, and Pearson r = 0.845, P-value = 0.001, respectively; Figure S2A and S2B). In addition, *Foxo3*, another isoform of FOXO, was upregulated in Hypox group, and its expression also positively correlated with *Foxo1* expression in Hypox group (Pearson r = 0.965, P-value < 0.0001; Figure S2C). Therefore, we summarized the DEGs of FOXO target genes in Figure 2C. Among a total of 14 DEGs, 12 were upregulated in Hypox group including *Ddit4*, *Depp1*, CCAAT/enhancer binding protein delta (*Cebpd*), growth arrest and DNA-damage-inducible 45 gamma (*Gadd45g*), Kruppel-like factor 2 (*Klf2*), Kruppel-like factor 4 (*Klf4*), sestrin 1 (*Sesn1*), myostatin (*Mstn*), activating transcription factor 4 (*Atf4*) and unc-51 like kinase 1 (*Ulk1*). The wingless-type MMTV integration site family member 11 (*Wnt11*) and tumor necrosis factor (ligand) superfamily member 10 (*Tnfsf10*) gene expression was downregulated. At the protein level, FOXO1 tended to increase in the Hypox group (P-value = 0.072; Figure 2D). Upstream of FOXO, hypoxia decreased insulin receptor substrate 1 (*Irs1*) as well as phosphoinositide-3-kinase regulatory subunit 3 (*Pik3r3*) expression (Figure 2E). These genes influence FOXO by stimulating AKT and the PI3K-AKT pathway, which was enriched in KEGG pathway analysis (31) using all DEGs (Table S2). However, the gene expression of any of the isoforms of AKT (*Akt1*, *Akt2* and *Akt3*) and AKT protein level were not changed (Figure 2E and 2F). However, phosphorylated AKT (p-AKT; S473) levels were decreased in the Hypox group, resulting in a lower p-AKT/AKT ratio (Figure 2F), suggesting less inhibition of FOXO1. These data further confirmed the suppression of PI3K-AKT pathway leading to FOXO1 activation in the Hypox group.

Based on the obtained results, we mapped the potential FOXO signaling pathway and further linked the FOXO target genes to their downstream genes in Figure 3. These genes and their interrelationships were based on KEGG pathway analysis (31) supplemented with literature (15). Next to the downregulated *Irs1* and *Pik3r3* in PI3K-AKT pathway, two other upstream FOXO regulators are serum/glucocorticoid regulated kinase 1 (*Sgk1*), inhibiting FOXO, and CREB binding protein (*Crebbp*), stimulating FOXO. *Sgk1* and *Crebbp* were both upregulated in Hypox group (Log2FC = 0.81, adjusted P-value < 0.0001 and Log2FC = 0.35, adjusted P-value < 0.0001, respectively). The regulated FOXO1 target genes were related to proteostasis (*Sesn1*, *Cebpd*, *Mstn*, *Atf4* and *Ddit4*), autophagy (*Depp1* and *Ulk1*), apoptosis (*Tnfsf10*,

Gadd45g, *Klf2* and *Klf4*) and muscle differentiation (*Wnt11*). Most DEGs related to proteostasis and autophagy were upregulated suggesting increased ALP (e.g. *Ulk1* and *Sqstm1*) and UPS (e.g. *Fbxo32* and *Trim63*) facilitating protein degradation. *Ddit4*, AKT1 substrate 1 (*Akt1s1*), and 4E-BP1 (*Eif4ebp1*) were also upregulated suggesting reduced activity of mTORC1 and reduced protein synthesis. In addition to these results, KEGG pathway analysis (31) shows regulation of Autophagy – animal, Protein processing in endoplasmic reticulum, Ribosome, Spliceosome, and Proteasome pathways (Table S2), and among these pathways most genes were upregulated in the Hypox mice (Figure S3, S4 and S5). Most DEGs of the WNT pathway were downregulated indicating inhibited development (differentiation) of skeletal muscle in the Hypox group. Additionally, the pathway regulating caspase 8 (*Casp8*) and caspase 7 (*Casp7*) were downregulated (Figure 3) suggesting suppressed apoptosis. To conclude, the 6-hour hypoxia activates the FOXO pathway resulting in increased protein degradation via UPS and ALP and reduced protein synthesis, which could influence skeletal muscle development in these young mice. Therefore, we further investigated the impact of hypoxia on proteotasis.

Six-hour hypoxia disturbed muscle proteostasis toward protein degradation

To further investigate the effect of hypoxia on muscle proteostasis, all DEGs involved were examined and summarized (Figure 4A). Twenty out of the total 23 DEGs involved in both protein synthesis and degradation were upregulated in the Hypox group. Among these DEGs, *Ddit4* was the most upregulated one (confirmed by Q-PCR; Figure 1D). However, DDIT4 protein level was not affected (Figure 4B).

Next, two main targets of the protein synthesis mTORC1 pathway, S6K and 4E-BP1, were investigated. Hypoxia decreased phosphorylated S6K (p-S6K; T389) and thereby p-S6K/S6K level (Figure 4C). Although hypoxia upregulated *Eif4ebp1,* 4E-BP1 protein level was not changed (P-value = 0.067; Figure 4D), the phosphorylated 4E-BP1 (p-4E-BP1; T37/46) and p-4E-BP1/4E-BP1 ratio were decreased in the Hypox group. These reduced phosphorylation level of S6K and 4E-BP1 was further confirmed by decreased phosphorylated mTOR (p-mTOR; S2448) (Figure S6), which altogether show decreased mTOR activity.

As skeletal muscle is a major reservoir of amino acids, serum amino acid levels of 32 different amino acids and derivatives were analyzed (Table S3). A total of 13 amino acids were regulated in Hypox group, of these 4 are essential amino acids. Histidine, leucine and phenylalanine were increased while methionine was decreased. An increase of 3 out of 4 changed essential amino acids in serum after 6-hour hypoxia exposure in the fasted state suggests enhanced protein degradation (32).

Out of all the DEGs related to proteostasis (Figure 4A), *Cebpd* was the second most regulated gene. *Cebpd* is involved in protein degradation and activates the atrophy markers *Fbxo32* and *Trim63* (Figure 3). The gene expressions of *Cebpd*, *Fbxo32* and *Trim63* were increased in the Hypox group (Figure 4A). The level of FBXO32 protein, an early atrophy response protein (33), was increased in Hypox group (Figure 5A) and showed a positive correlation with FOXO1 protein expression levels (Pearson r = 0.978, P-value = 0.001; Figure 5B). This suggests that 6-hour hypoxia exposure activated FBXO32 via FOXO1 to initiate protein degradation. As the final part of UPS, 16 proteasome genes were significantly upregulated in KEGG enrichment analysis in the Hypox group (Figure S5). TRIM63 protein level (Figure 5C) and total ubiquitinated protein (Figure 5D) were not affected in the Hypox group, suggesting that 6 hours of hypoxia may have been too short to also activate these protein degradation responses.

The disturbed proteostasis upon 6-hour hypoxia also include the activation of unfolded protein response (UPR) in Gene Ontology-Biological Process (34). Of the 11 UPR-involved DEGs, 10 DEGs were

upregulated in Hypox group (Figure S7). Among these upregulated DEGs, transcription factor 3 (*Atf3*) and protein phosphatase 1 regulatory subunit 15A (*Ppp1r15a*) are targets of transcription factor 4 (ATF4), of which the gene expression was increased in Hypox group as the 4th most upregulated gene (Figure S7). ATF4 was enriched as transcription factor (P-value = 0.002) in Gene Set Enrichment Analysis with MSigDB gene list, further suggesting the activation of ATF4 by hypoxia. Interestingly, a positive correlation was only found in the Hypox group between *Atf4* and FOXO1 (Pearson r = 0.752, P-value = 0.085; Figure 6A), *Eif4ebp1* (Pearson r = 0.632, P-value = 0.028; Figure 6B), *Ddit4* (Pearson r = 0.609, P-value = 0.036; Figure 6C) and *Depp1* (Pearson r = 0.654, P-value = 0.021), and FBXO32 (Pearson r = 0.783, P-value = 0.065; Figure 6D). FOXO1 has been shown a regulator of ATF4 (35), suggesting that FOXO1 may have activated ATF4 after 6-hour hypoxia.

DISCUSSION

Long-term hypoxia has been shown to reduce skeletal muscle mass in adults by increasing protein degradation over protein synthesis (36). Whether these pathways were already affected by short-term (acute) hypoxia in the growing skeletal muscle of young mice remained to be determined. Therefore, we investigated the *in vivo* response of acute hypoxia on muscle proteostasis in *M. gastrocnemius* of 24-day-old mice. Our results showed that 6-hour hypoxia (12% O_2) induced a hypoxic response in skeletal muscle by increasing expression of HIF1 and FOXO1 target genes (*Ankrd37*, *Ddit4* and *Depp1*). Similarly, an increased *Ddit4* and *Depp1* expression were also observed in *M. gastrocnemius* of adult mice after 6-hour hypoxia (12% O_2) (15). This suggests that activation of the FOXO1 pathway in skeletal muscle upon acute hypoxia exposure occurs throughout different ages, including the important early stage of skeletal muscle growth and development. Due to its role in regulating the balance between protein synthesis and breakdown, the FOXO1 activation upon 6-hour hypoxia could already have significant impact on these processes. Aligned with this, the early muscle atrophy marker FBXO32 (33) was increased. However, TRIM63, another muscle atrophy marker contributing to sustained muscle breakdown (37), was not changed despite the upregulation of *Trim63*. In addition, total protein ubiquitination levels were not increased, which suggests that a 6-hour environmental hypoxia increases early muscle atrophy, but that a longer hypoxia exposure or a later timepoint of analysis may be needed to observe an increase in total protein ubiquitination and subsequently decreased muscle mass. One of the reasons could be that the substrates of FBXO32 are not yet post-translationally modified after 6-hour hypoxia, which is required for F-box proteins ubiquitination (38). Similar results were found in longer hypoxic exposures. For example, de Thije *et al.* observed decreased weight of *M. gastrocnemius* accompanied with increased *Fbxo32* and *Trim63* expression after a 3-day hypoxia (8% O_2) in 12-week-old mice (39). Our results are also in line with the results of Fu *et al*. who also observed increased nuclear FOXO1 and FBXO32 expression but unchanged total protein ubiquitination after 4-week hypoxia (12.4% O_2) in rats (10). FOXO1 activated FBXO32 that plays a role in protein degradation via UPS as an E3 ubiquitin ligase. In addition to UPS, FOXO1 also promotes protein degradation via ALP by increasing the expression of autophagy-related genes (40). This is suggested by the upregulation of genes such as *Ankrd37*, *Depp1*, *Ulk1* and *Map1lc3a (Lc3a)*. This is further supported by the study of Giordano *et al.* who observed that 4-day intermittent hypoxia (6% O_2) induced atrophy and increased LC3B in *diaphragm* of 8-week-old mice. Overall, our results suggests that protein breakdown is initiated in the *M. gastrocnemius* within 6-hour environmental hypoxia. As skeletal muscle is a major protein deposit, the increased serum levels of the essential amino acids leucine, a branched-chain amino acid (BCAA), histidine and phenylalanine in fasted state support increased protein degradation. Similarly, Muratsubaki and Yamaki also observed

increased BCAAs and phenylalanine in serum of 8-week-old rat after 5-hour hypoxia (9.4% O_2) (41). Since serum levels of tyrosine, a product of phenylalanine, was not affected, amino acid and protein synthesis might also be reduced next to increased protein breakdown.

This reduced protein synthesis upon 6-hour hypoxia exposure is supported by changes found in the AKT-mTORC1 pathway. Decreased AKT phosphorylation has been showed as acute hypoxia response by Gan *et al.* after 2-hour hypoxia (8% O_2) (14). In this study, the reduced AKT phosphorylation led to decreased mTORC1 activity and resulted in decreased p-4E-BP1/4E-BP1, p-S6K/S6K and p-mTOR by p-S6K. This is in line with published results of 12-day hypoxia (8% O_2) exposure that decreased p-mTOR in mouse *M. gastrocnemius* (42). The decreased mTORC1 activity also indicated by increased serum phenylalanine, which has been found in 72-hour fasted humans (43). In addition to AKT, hypoxia also inhibits mTORC1 activity via increased DDIT4, the target gene of FOXO1 (44). However, in this study, the increased *Ddit4* expression did not lead to higher DDIT4 protein level in Hypox mice. This may be due to the pre-activation of FOXO1 and DDIT4 by the 6-hour fasting prior to hypoxia exposure (35) and the long stability of DDIT4 over 2 days *in vitro* (45). In this way, FOXO1 and DDIT4 might already be increased before a hypoxia exposure, of which only FOXO1 and *Ddit4* expression further increased by hypoxia. In addition, FOXO1 also upregulated *Atf4* leading to increased downstream *Ppp1r15a* and *Eif4ebp1* engaging in unfolded protein response and mTORC1, separately. Similarly, Kiesel *et al.* also observed hypoxia-mediated ATF4 activation in murine mammary cancer cell, which further promoted survival (46).

Altogether, our data showed that 6-hour physiological plausible environmental hypoxia decreased AKT-mTORC1 and activated FOXO1 towards protein degradation where FOXO1 played a central role (Figure 7) suggesting a possible impact on decreasing in muscle mass. The effects of hypoxia are likely caused by energy stress, which is supported by increased BCAA and other essential amino acids released in serum suggesting increased catabolism, upregulated expression of genes associated with glycolysis (Figure S8), and having Ribosome, Spliceosome and Protein processing in Endoplasmic reticulum among the top-10 regulated non-disease KEGG pathways. Such disturbed proteostasis by might be influenced by hypoxia-induced signals due to the whole-body hypoxia exposure. Since glucose was not different (Figure 1C), we did not further analyze insulin or glucagon. In addition to growth factor signaling, steroid may play a role. For example, 4-day hypoxia (8% O_2) of 12-week-old mice has been shown to increase levels of corticosterone, the main glucocorticoid in rodents (39). Similarly, intermittent hypoxia (12% O_2, 8 hours per day) induced corticosterone in rats from the first day of exposure and kept increasing until the fourth day (47). In turn, the increased corticosterone level correlated to increased protein degradation in skeletal muscle via activating glucocorticoid receptor (48). It is therefore of interest to examine the role of glucocorticoids in future studies.

As skeletal muscles of 24-day-old mice are still hypertrophic requiring energy for protein synthesis, the hypoxia-induced energy shortage could postpone the muscle development, which is supported by downregulated genes in WNT pathway. WNT11 and FZD6 promote skeletal muscle formation and regeneration (49). This downregulation of the WNT pathway is further associated with downregulated Rac family small GTPase 2 (*Rac2*), Rho-associated coiled-coil containing protein kinase 1 (*Rock1*) and *Rock2* (50). Their downstream motor protein gene expressions were also changed, with downregulated myosin light polypeptide kinase (*Mylk*; myosin heavy chain 7B (*Myh7b*; type I myofiber) and upregulated myosin light chain, phosphorylatable (*Mylpf*; type II myofiber) suggesting the trend of type I to type II myofiber transition. This is in line with decreased type I myofiber number in muscle specific FOXO1 overexpression mouse model (51).

In summary, we newly showed that six-hour hypoxia increased protein degradation via activating FOXO1 signaling and decreased protein synthesis via inhibiting AKT-mTORC1 in *M. gastrocnemius* of 24-day-old mice (Figure 7). This can cause premature muscle atrophy. In addition, gene expression changes indicated alterations in skeletal muscle structure. Together the changes observed could potentially hamper muscle development of young mice. We were unable to obtain substantiating morphological evidence, because changes in muscle mass and structure after 6-hour hypoxia exposure are likely too little to be analyzed. Whether the acute adverse hypoxia at early life impact on muscle function in later life should be further investigated. McDonald *et al.* showed that chronic intermittent hypoxia in 3-week-old rats decreased sternohyoid muscle force, which persisted into young adult life (42 days) (52). If the persistent damage caused by hypoxia also happens in mouse skeletal muscle, then it would be relevant to analyze the effect of acute hypoxia, in view of habitual environmental hypoxia challenges such as high altitude holidays or even airflights, on skeletal muscle development of especially infants and children. Also, aging can be associated with shortage of body oxygen availability mostly due to a diminished lung function, and it would be interesting to see if this contributes or exacerbates muscle loss observed in aging.

DATA AVAILABILITY

RNA-Seq data were deposited in Gene Expression Omnibus (GEO) with accession ID: GSE255522. Upon submission, authors agree to make any materials, data, and associated protocols available upon request.

SUPPLEMENTAL MATERIAL

Figure S1 – S8 https://doi.org/10.6084/m9.figshare.28497629.v1

Table S1 – S3 https://doi.org/10.6084/m9.figshare.28497698.v1

ACKNOWLEDGMENTS

The authors gratefully acknowledge all help at small animal facility (CKP) of the Wageningen University Animal facility CARUS for mouse caring and dissection. The authors also thank all members of the Department of Human and Animal Physiology for their helpful contributions, especially Anna F. Bekebrede and Gerwin Smits for helping RNA-Seq analysis, Evert M. van Schothorst for uploading RNA-Seq data and Chris Klein and Jinmeng Yang for helping animal experiment. Ferran Fos Codoñer for helping graphical abstract.

GRANTS

China Scholarship Council, Grant Number: 201908110278 (to JS).

DISCLOSURES

The authors declare no competing interests.

AUTHOR CONTRIBUTIONS

JS, MJ, CC, JK and SG conceived and designed research. JS, MJ, CC , VB and NW performed experiments. JS, VB and NW analyzed data. JS, JK and SG interpreted results of experiments. JS, SG and JK prepared

figures, drafted manuscript, edited and revised manuscript. All authors approved final version of manuscript.

FIGURE LEGENDS

Figure 1: Increased HIF1 and FOXO1 signaling in *M. gastrocnemius* after six hours exposure to hypoxia (Hypox; 12% O_2) versus normoxia (Norm). Body weight (A) and lean mass (B) of the mice before exposure, (C) blood glucose levels directly after Norm or Hypox. (D) *Ankrd37*, *Ddit4* and *Depp1* relative gene expression. (E) Correlations between *Ddit4*, *Depp1* and *Ankrd37* relative gene expression. Values are presented as mean ± SD, n = 11-12 per group, ** P-value < 0.01, *** P-value < 0.001.

Figure 2: Six hours hypoxia (12% O_2) activated FOXO signaling pathway and its effect on transcriptional level in *M. gastrocnemius*. (A) 3D PCA plot shows gene expression of Euclidean distance between samples on Log transformed data. (B) All expressed genes with an Entrez annotation are displayed in a volcano plot based on their Log2 fold change (Log2FC) and adjusted P-value. Dashed lines indicate adjusted P-value < 0.05 cutoff and Log2FC = 0. Non-regulated, upregulated, and downregulated genes are labelled in grey, red, and blue respectively. (C) Heatmap showing FOXO1 and FOXO3 target genes. (D) Western blot analysis of FOXO1. (E) RNA-Seq normalized counts of *Irs1*, *Pik3r3*, *Akt1*, *Akt2* and *Akt3*. (F) Western blot analysis of total AKT, p-AKT (S473). Values are presented as mean ± SD, n = 6 (western blot) or 12 (RNA-Seq) per group, * P-value < 0.05, ** P-value < 0.01.

Figure 3: Potential regulated pathway indicating central role of FOXO1 after 6-hour hypoxia.

Figure 4: Six hours hypoxia (12% O_2) affected protein synthesis by decreasing 4E-BP1 and S6K phosphorylation. (A) Heatmap showing DEGs involved in proteostasis in Hypox (12% O_2) versus Norm. Western blot analysis of DDIT4 (B), S6K and p-S6K (T389) (C), 4E-BP1 and p-4E-BP1 (T37/46) (D). Values are presented as mean ± SD, n = 5-6 (western blot) or 12 (RNA-Seq) per group, * P-value < 0.05, ** P-value < 0.01.

Figure 5: Six hours hypoxia (12% O_2) increased FBXO32 via FOXO1 pathway. (A) Western blot analysis of FBXO32. (B) Correlations between protein levels of FBXO32 and FOXO1. Western blot analysis of TRIM63 (C) and total ubiquitinated protein (D). Values are presented as mean ± SD, n = 6 per group, * P-value < 0.05.

Figure 6: FOXO1 activation promoted *Atf4* and ATF4 target gene expression under hypoxia. Correlations between *Atf4* expression and FOXO1 protein level (A), *Eif4ebp1* expression (B), *Ddit4* and *Depp1* expression (C) and FBXO32 and expression (D), n = 6 (western blot) or 12 (RNA-Seq).

Figure 7: Six hours hypoxia (12% O_2) showed decreased proteostasis by increasing FBXO32 via FOXO1 and decreasing p-4E-BP1 and p-S6K via AKT-mTOR pathway in *M. gastrocnemius*.

REFERENCES

1. **Rolfe DF, and Brown GC**. Cellular energy utilization and molecular origin of standard metabolic rate in mammals. *Physiol Rev* 77: 731-758, 1997. https://doi.org/10.1152/physrev.1997.77.3.731.
2. **Wang P, Holst C, Wodzig WK, Andersen MR, Astrup A, van Baak MA, Larsen TM, Jebb SA, Kafatos A, Pfeiffer AF, Martinez JA, Handjieva-Darlenska T, Kunesova M, Viguerie N, Langin D, Saris WH, Mariman EC, and Diogenes c**. Circulating ACE is a predictor of weight loss maintenance not only in overweight and obese women, but also in men. *Int J Obes (Lond)* 36: 1545-1551, 2012. https://doi.org/10.1038/ijo.2011.278.
3. **Zurlo F, Larson K, Bogardus C, and Ravussin E**. Skeletal-muscle metabolism is a major determinant of resting energy-expenditure. *J Clin Invest* 86: 1423-1427, 1990. https://doi.org/10.1172/Jci114857.
4. **Lindqvist LM, Tandoc K, Topisirovic I, and Furic L**. Cross-talk between protein synthesis, energy metabolism and autophagy in cancer. *Curr Opin Genet Dev* 48: 104-111, 2018. https://doi.org/10.1016/j.gde.2017.11.003.
5. **Slot IG, Schols AM, de Theije CC, Snepvangers FJ, and Gosker HR**. Alterations in skeletal muscle oxidative phenotype in mice exposed to 3 weeks of normobaric hypoxia. *J Cell Physiol* 231: 377-392, 2016. https://doi.org/10.1002/jcp.25083.
6. **Debevec T, Ganse B, Mittag U, Eiken O, Mekjavic IB, and Rittweger J**. Hypoxia aggravates inactivity-related muscle wasting. *Front Physiol* 9: 494, 2018. https://doi.org/10.3389/fphys.2018.00494.
7. **Bodine SC, Stitt TN, Gonzalez M, Kline WO, Stover GL, Bauerlein R, Zlotchenko E, Scrimgeour A, Lawrence JC, Glass DJ, and Yancopoulos GD**. Akt/mTOR pathway is a crucial regulator of skeletal muscle hypertrophy and can prevent muscle atrophy. *Nat Cell Biol* 3: 1014-1019, 2001. https://doi.org/10.1038/ncb1101-1014.
8. **Sanchez AM, Candau RB, and Bernardi H**. FoxO transcription factors: their roles in the maintenance of skeletal muscle homeostasis. *Cell Mol Life Sci* 71: 1657-1671, 2014. https://doi.org/10.1007/s00018-013-1513-z.
9. **Laplante M, and Sabatini DM**. mTOR signaling in growth control and disease. *Cell* 149: 274-293, 2012. https://doi.org/10.1016/j.cell.2012.03.017.
10. **Fu P, Zhu R, Gao W, and Gong L**. Effects of resistance training on alleviating hypoxia-induced muscle atrophy: Focus on acetylation of FoxO1. *J Cell Mol Med* 28: e18096, 2024. https://doi.org/10.1111/jcmm.18096.
11. **Attaix D, Ventadour S, Codran A, Bechet D, Taillandier D, and Combaret L**. The ubiquitin-proteasome system and skeletal muscle wasting. *Essays Biochem* 41: 173-186, 2005. https://doi.org/10.1042/EB0410173.
12. **Bodine SC, Latres E, Baumhueter S, Lai VK, Nunez L, Clarke BA, Poueymirou WT, Panaro FJ, Na E, Dharmarajan K, Pan ZQ, Valenzuela DM, DeChiara TM, Stitt TN, Yancopoulos GD, and Glass DJ**. Identification of ubiquitin ligases required for skeletal muscle atrophy. *Science* 294: 1704-1708, 2001. https://doi.org/10.1126/science.1065874.
13. **Dukhande VV, Sharma GC, Lai JC, and Farahani R**. Chronic hypoxia-induced alterations of key enzymes of glucose oxidative metabolism in developing mouse liver are mTOR dependent. *Mol Cell Biochem* 357: 189-197, 2011. https://doi.org/10.1007/s11010-011-0889-z.

14. **Gan Z, Powell FL, Zambon AC, Buchholz KS, Fu Z, Ocorr K, Bodmer R, Moya EA, Stowe JC, Haddad GG, and McCulloch AD**. Transcriptomic analysis identifies a role of PI3K-Akt signalling in the responses of skeletal muscle to acute hypoxia in vivo. *J Physiol* 595: 5797-5813, 2017. https://doi.org/10.1113/JP274556.
15. **Song JY, Duivenvoorde LPM, Grefte S, Kuda O, Martínez-Ramírez F, van der Stelt I, Mastorakou D, van Schothorst EM, and Keijer J**. Normobaric hypoxia shows enhanced FOXO1 signaling in obese mouse muscle linked to metabolism and muscle structure and neuromuscular innervation. *Pflug Arch Eur J Phy* 475: 1265-1281, 2023. https://doi.org/10.1007/s00424-023-02854-4.
16. **Gokhin DS, Ward SR, Bremner SN, and Lieber RL**. Quantitative analysis of neonatal skeletal muscle functional improvement in the mouse. *J Exp Biol* 211: 837-843, 2008. https://doi.org/10.1242/jeb.014340.
17. **Ontell M, Feng KC, Klueber K, Dunn RF, and Taylor F**. Myosatellite cells, growth, and regeneration in murine dystrophic muscle: a quantitative study. *Anat Rec* 208: 159-174, 1984. https://doi.org/10.1002/ar.1092080203.
18. **White RB, Bierinx AS, Gnocchi VF, and Zammit PS**. Dynamics of muscle fibre growth during postnatal mouse development. *BMC Dev Biol* 10: 21, 2010. https://doi.org/10.1186/1471-213X-10-21.
19. **Bachman JF, Klose A, Liu W, Paris ND, Blanc RS, Schmalz M, Knapp E, and Chakkalakal JV**. Prepubertal skeletal muscle growth requires Pax7-expressing satellite cell-derived myonuclear contribution. *Development* 145: dev167197, 2018. https://doi.org/10.1242/dev.167197.
20. **Bayol SA, Bruce CR, and Wadley GD**. Growing healthy muscles to optimise metabolic health into adult life. *J Dev Orig Hlth Dis* 5: 420-434, 2014. https://doi.org/10.1017/S2040174414000452.
21. **Börsch A, Ham DJ, Mittal N, Tintignac LA, Migliavacca E, Feige JN, Rüegg MA, and Zavolan M**. Molecular and phenotypic analysis of rodent models reveals conserved and species-specific modulators of human sarcopenia. *Commun Biol* 4: 2021. https://doi.org/10.1038/s42003-021-01723-z.
22. **Andrews S**. FastQC: A Quality Control Tool for High Throughput Sequence Data [Online]. Available online at: http://www.bioinformatics.babraham.ac.uk/projects/fastqc/: 2015.
23. **Dobin A, Davis CA, Schlesinger F, Drenkow J, Zaleski C, Jha S, Batut P, Chaisson M, and Gingeras TR**. STAR: ultrafast universal RNA-seq aligner. *Bioinformatics* 29: 15-21, 2013. https://doi.org/10.1093/bioinformatics/bts635.
24. **Anders S, Pyl PT, and Huber W**. HTSeq--a Python framework to work with high-throughput sequencing data. *Bioinformatics* 31: 166-169, 2015. https://doi.org/10.1093/bioinformatics/btu638.
25. **Love MI, Huber W, and Anders S**. Moderated estimation of fold change and dispersion for RNA-seq data with DESeq2. *Genome Biol* 15: 550, 2014. https://doi.org/10.1186/s13059-014-0550-8.
26. **Bekebrede AF, de Boer VCJ, Gerrits WJJ, and Keijer J**. Functional and molecular profiling of fasted piglets reveals decreased energy metabolic function and cell proliferation in the small intestine. *Bba-Bioenergetics* 1863: 97-97, 2022. https://doi.org/10.1016/j.bbabio.2022.148872.
27. **Ye J, Coulouris G, Zaretskaya I, Cutcutache I, Rozen S, and Madden TL**. Primer-BLAST: A tool to design target-specific primers for polymerase chain reaction. *Bmc Bioinformatics* 13: 134, 2012. https://doi.org/10.1186/1471-2105-13-134.
28. **Schindelin J, Arganda-Carreras I, Frise E, Kaynig V, Longair M, Pietzsch T, Preibisch S, Rueden C, Saalfeld S, Schmid B, Tinevez JY, White DJ, Hartenstein V, Eliceiri K, Tomancak P, and Cardona A**. Fiji: an open-source platform for biological-image analysis. *Nat Methods* 9: 676-682, 2012. https://doi.org/10.1038/nmeth.2019.
29. **Gray N, Zia R, King A, Patel VC, Wendon J, McPhail MJ, Coen M, Plumb RS, Wilson ID, and Nicholson JK**. High-speed quantitative UPLC-MS analysis of multiple amines in human plasma and serum via precolumn derivatization with 6-aminoquinolyl-N-hydroxysuccinimidyl carbamate: application to acetaminophen-induced liver failure. *Anal Chem* 89: 2478-2487, 2017. https://doi.org/10.1021/acs.analchem.6b04623.

30. **Hoevenaars FPM, Keijer J, van der Stelt I, Duivenvoorde LPM, Herreman L, van Nes R, Friedecký D, Hegeman MA, and van Schothorst EM**. White adipose tissue response of obese mice to ambient oxygen restriction at thermoneutrality: response markers identified, but no WAT inflammation. *Genes (Basel)* 10: 359, 2019. https://doi.org/10.3390/genes10050359.
31. **Kanehisa M, Furumichi M, Sato Y, Kawashima M, and Ishiguro-Watanabe M**. KEGG for taxonomy-based analysis of pathways and genomes. *Nucleic Acids Res* 51: D587–D592, 2022. https://doi.org/10.1093/nar/gkac963.
32. **Imai D, Nakanishi N, Shinagawa N, Yamamoto S, Ichikawa T, Sumi M, Matsui T, Hosomi Y, Hasegawa Y, Munekawa C, Miyoshi T, Okamura T, Kitagawa N, Hashimoto Y, Okada H, Sakui N, Sasano R, Hamaguchi M, and Fukui M**. Association of elevated serum branched-chain amino acid levels with longitudinal skeletal muscle loss. *J Endocr Soc* 8: bvad178, 2024. https://doi.org/10.1210/jendso/bvad178.
33. **Ninfali C, Siles L, Darling DS, and Postigo A**. Regulation of muscle atrophy-related genes by the opposing transcriptional activities of ZEB1/CtBP and FOXO3. *Nucleic Acids Res* 46: 10697-10708, 2018. https://doi.org/10.1093/nar/gky835.
34. **Ashburner M, Ball CA, Blake JA, Botstein D, Butler H, Cherry JM, Davis AP, Dolinski K, Dwight SS, Eppig JT, Harris MA, Hill DP, Issel-Tarver L, Kasarskis A, Lewis S, Matese JC, Richardson JE, Ringwald M, Rubin GM, and Sherlock G**. Gene ontology: tool for the unification of biology. The Gene Ontology Consortium. *Nat Genet* 25: 25-29, 2000. https://doi.org/10.1038/75556.
35. **Oyabu M, Takigawa K, Mizutani S, Hatazawa Y, Fujita M, Ohira Y, Sugimoto T, Suzuki O, Tsuchiya K, Suganami T, Ogawa Y, Ishihara K, Miura S, and Kamei Y**. FOXO1 cooperates with C/EBPdelta and ATF4 to regulate skeletal muscle atrophy transcriptional program during fasting. *FASEB J* 36: e22152, 2022. https://doi.org/10.1096/fj.202101385RR.
36. **Chaillou T, Koulmann N, Meunier A, Pugniere P, McCarthy JJ, Beaudry M, and Bigard X**. Ambient hypoxia enhances the loss of muscle mass after extensive injury. *Pflugers Arch* 466: 587-598, 2014. https://doi.org/10.1007/s00424-013-1336-7.
37. **Peris-Moreno D, Taillandier D, and Polge C**. MuRF1/TRIM63, master regulator of muscle mass. *Int J Mol Sci* 21: 2020. https://doi.org/10.3390/ijms21186663.
38. **Nguyen KM, and Busino L**. *The biology of F-box proteins: the SCF family of E3 ubiquitin ligases*. 2020, p. 111-122.
39. **De Theije CC, Schols AMWJ, Lamers WH, Ceelen JJM, Van Gorp RH, Rob Hermans JJ, Elonore Köhler S, and Langen RCJ**. Glucocorticoid receptor signaling impairs protein turnover regulation in hypoxia-induced muscle atrophy in male mice. *Endocrinology* 159: 519-534, 2018. https://doi.org/10.1210/en.2017-00603.
40. **Liang R, Liu N, Cao JL, Liu TL, Sun P, Cai XH, Zhang LQ, Liu YJ, Zou JQ, Wang L, Ding XJ, Zhang BY, Shen ZY, Yoshida S, Dou J, and Wang SS**. HIF-1α/FOXO1 axis regulated autophagy is protective for β cell survival under hypoxia in human islets. *Bba-Mol Basis Dis* 1868: 2022. https://doi.org/10.1016/j.bbadis.2022.166356.
41. **Muratsubaki H, and Yamaki A**. Profile of plasma amino acid levels in rats exposed to acute hypoxic hypoxia. *Indian J Clin Biochem* 26: 416-419, 2011. https://doi.org/10.1007/s12291-011-0125-3.
42. **de Theije CC, Schols A, Lamers WH, Neumann D, Kohler SE, and Langen RCJ**. Hypoxia impairs adaptation of skeletal muscle protein turnover- and AMPK signaling during fasting-induced muscle atrophy. *Plos One* 13: e0203630, 2018. https://doi.org/10.1371/journal.pone.0203630.
43. **Vendelbo MH, Moller AB, Christensen B, Nellemann B, Clasen BFF, Nair KS, Jorgensen JOL, Jessen N, and Moller N**. Fasting increases human skeletal muscle net phenylalanine release and this is associated with decreased mTOR signaling. *Plos One* 9: e102031, 2014. https://doi.org/10.1371/journal.pone.0102031.

44. **Brugarolas J, Lei K, Hurley RL, Manning BD, Reiling JH, Hafen E, Witters LA, Ellisen LW, and Kaelin WG, Jr.** Regulation of mTOR function in response to hypoxia by REDD1 and the TSC1/TSC2 tumor suppressor complex. *Genes Dev* 18: 2893-2904, 2004. https://doi.org/10.1101/gad.1256804.
45. **Wang YJ, Han E, Xing QH, Yan J, Arrington A, Wang C, Tully D, Kowolik CM, Lu DM, Frankel PH, Zhai J, Wen W, Hone D, Yip MLR, and Yim JH**. Baicalein upregulates DDIT4 expression which mediates mTOR inhibition and growth inhibition in cancer cells. *Cancer Lett* 358: 170-179, 2015. https://doi.org/10.1016/j.canlet.2014.12.033.
46. **Kiesel VA, Sheeley MP, Hicks EM, Andolino C, Donkin SS, Wendt MK, Hursting SD, and Teegarden D**. Hypoxia-mediated ATF4 induction promotes survival in detached conditions in metastatic murine mammary cancer cells. *Front Oncol* 12: 767479, 2022. https://doi.org/10.3389/fonc.2022.767479.
47. **Hwang GS, Chen CC, Chou JC, Chang LL, Kan SF, Lai WH, Lieu FK, Hu S, Wang PS, and Wang SW**. Stimulatory effect of intermittent hypoxia on the production of corticosterone by zona fasciculata-reticularis cells in rats. *Scientific Reports* 7: 2017. https://doi.org/10.1038/s41598-017-07054-6.
48. **Sato AY, Richardson D, Cregor M, Davis HM, Au ED, McAndrews K, Zimmers TA, Organ JM, Peacock M, Plotkin LI, and Bellido T**. Glucocorticoids induce bone and muscle atrophy by tissue-specific mechanisms upstream of E3 ubiquitin ligases. *Endocrinology* 158: 664-677, 2017. https://doi.org/10.1210/en.2016-1779.
49. **Girardi F, and Le Grand F**. Wnt signaling in skeletal muscle development and regeneration. *Prog Mol Biol Transl Sci* 153: 157-179, 2018. https://doi.org/10.1016/bs.pmbts.2017.11.026.
50. **Zhang J, Ying ZZ, Tang ZL, Long LQ, and Li K**. MicroRNA-148a promotes myogenic differentiation by targeting the ROCK1 gene. *J Biol Chem* 287: 21093-21101, 2012. https://doi.org/10.1074/jbc.M111.330381.
51. **Kamei Y, Miura S, Suzuki M, Kai Y, Mizukami J, Taniguchi T, Mochida K, Hata T, Matsuda J, Aburatani H, Nishino I, and Ezaki O**. Skeletal muscle FOXO1 (FKHR) transgenic mice have less skeletal muscle mass, down-regulated Type I (slow twitch/red muscle) fiber genes, and impaired glycemic control. *J Biol Chem* 279: 41114-41123, 2004. https://doi.org/10.1074/jbc.M400674200.
52. **McDonald FB, Williams R, Sheehan D, and O'Halloran KD**. Early life exposure to chronic intermittent hypoxia causes upper airway dilator muscle weakness, which persists into young adulthood. *Exp Physiol* 100: 947-966, 2015. https://doi.org/10.1113/EP085003.

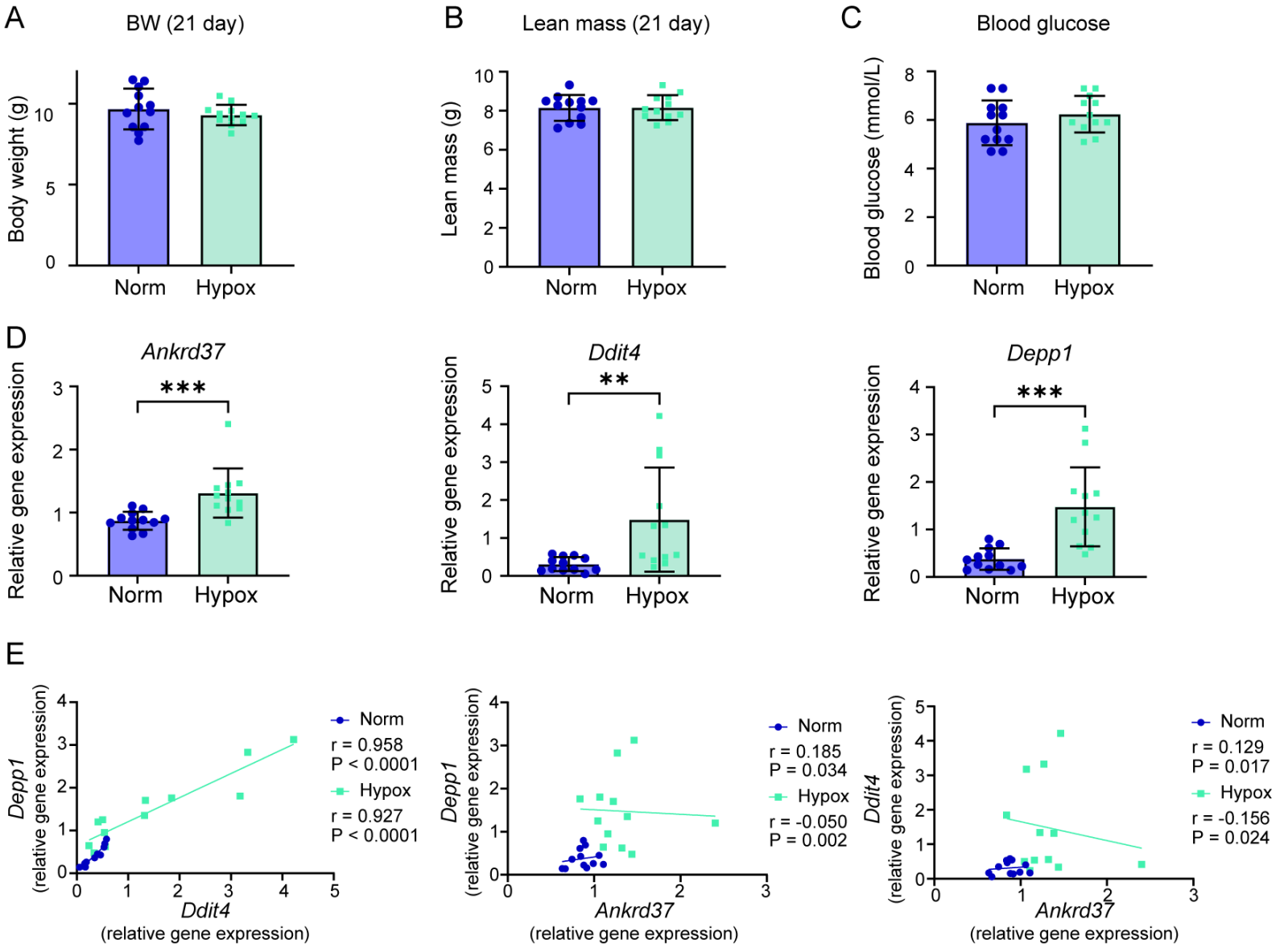
A
BW (21 day)
Body weight (g)
Norm
Hypox
B
Lean mass (21 day)
Lean mass (g)
C
Blood glucose
Blood glucose (mmol/L)
D
Ankrd37
Ddit4
Depp1
Relative gene expression
***
**
E
Depp1 (relative gene expression)
Ddit4 (relative gene expression)
Norm
r = 0.958
P < 0.0001
Hypox
r = 0.927
P < 0.0001
Ankrd37 (relative gene expression)
r = 0.185
P = 0.034
r = -0.050
P = 0.002
r = 0.129
P = 0.017
r = -0.156
P = 0.024

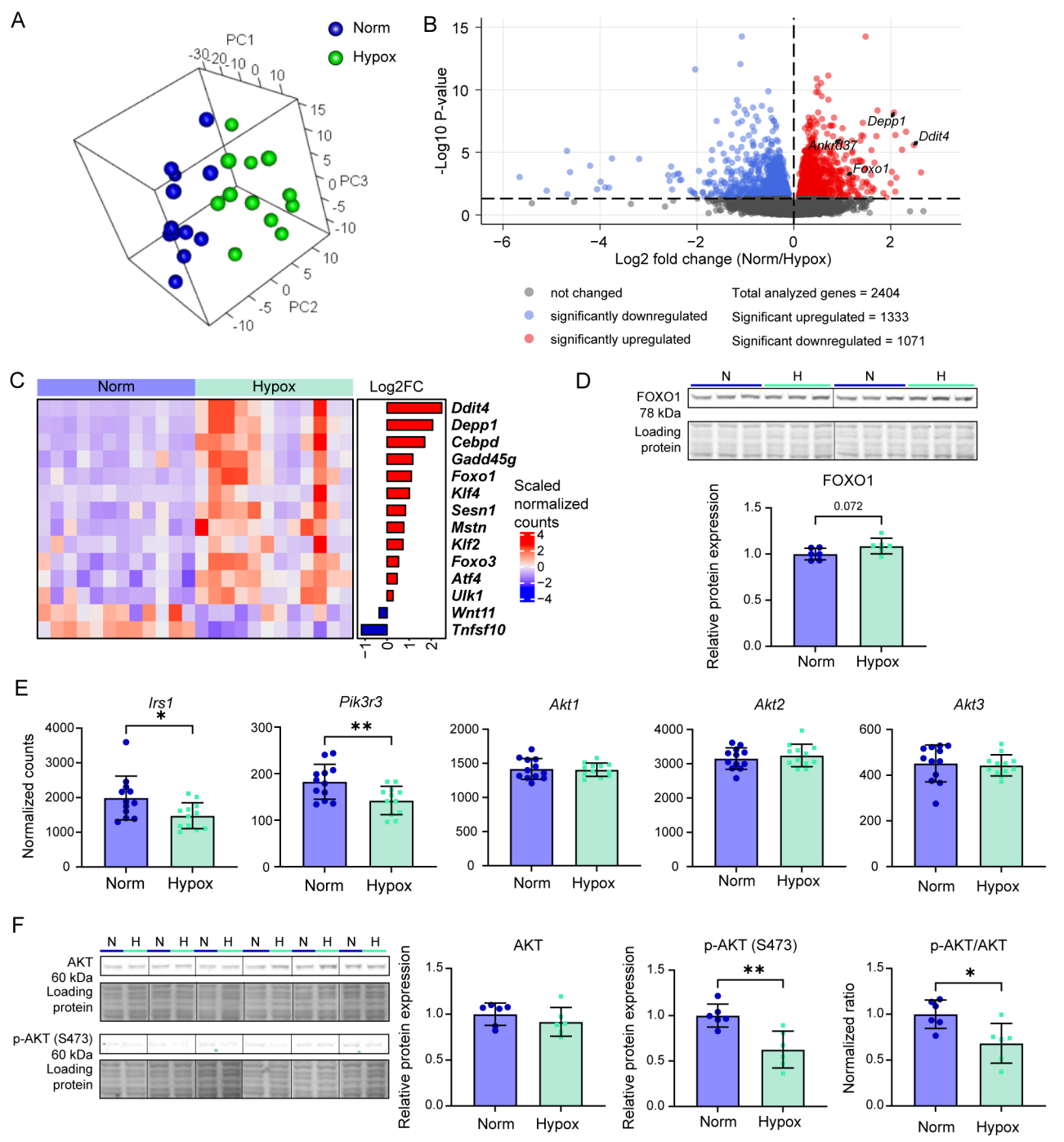
A
Norm
Hypox
PC1
PC2
PC3
B
-Log10 P-value
Log2 fold change (Norm/Hypox)
Depp1
Ddit4
Ankrd37
Foxo1
not changed
significantly downregulated
significantly upregulated
Total analyzed genes = 2404
Significant upregulated = 1333
Significant downregulated = 1071
C
Norm
Hypox
Log2FC
Ddit4
Depp1
Cebpd
Gadd45g
Foxo1
Klf4
Sesn1
Mstn
Klf2
Foxo3
Atf4
Ulk1
Wnt11
Tnfsf10
Scaled normalized counts
D
N
H
FOXO1 78 kDa
Loading protein
FOXO1
0.072
Relative protein expression
Norm
Hypox
E
Irs1
Pik3r3
Akt1
Akt2
Akt3
Normalized counts
F
AKT 60 kDa
p-AKT (S473) 60 kDa
Loading protein
AKT
p-AKT (S473)
p-AKT/AKT
Normalized ratio

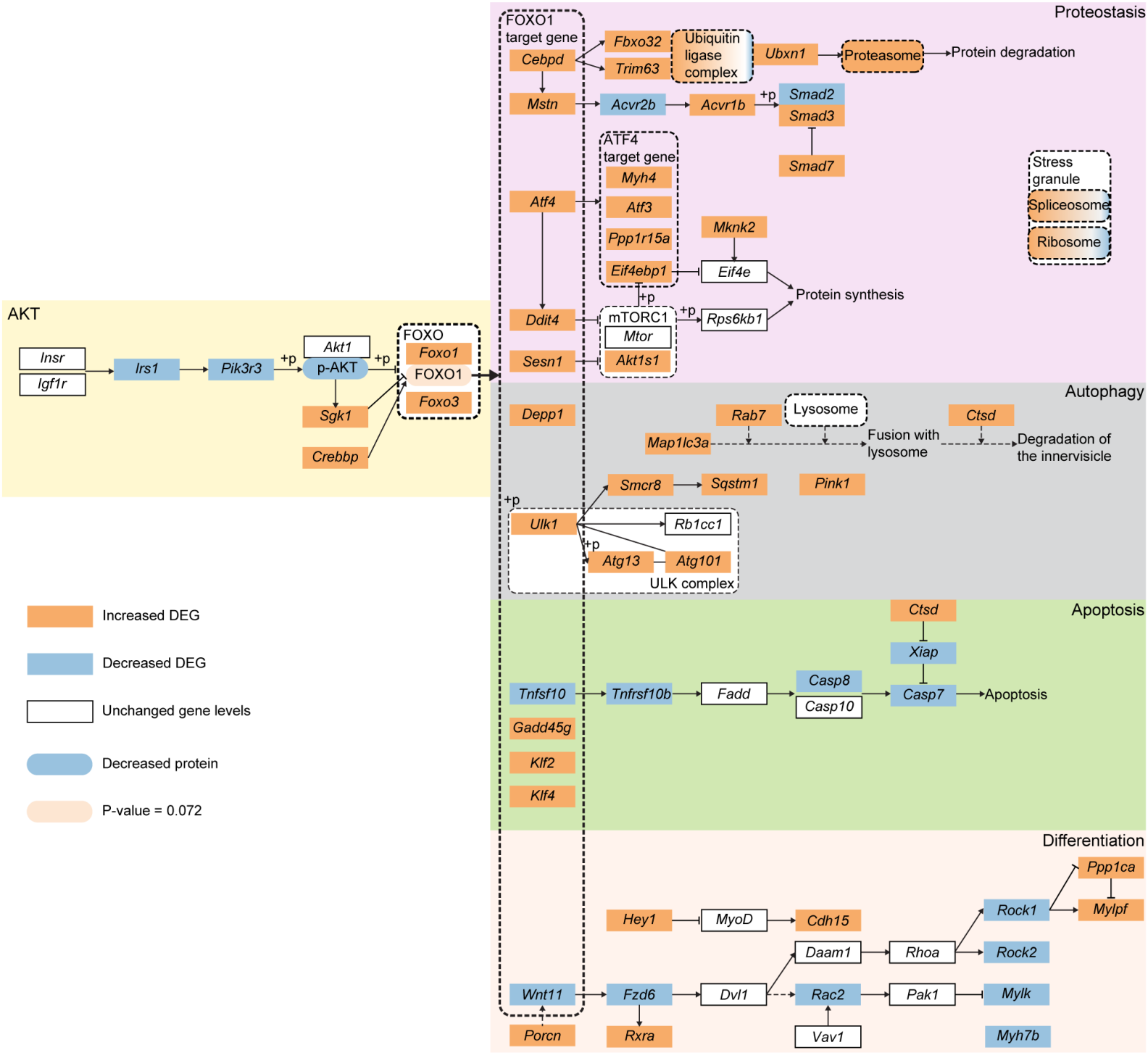
Proteostasis
FOXO1 target gene
Cebpd
Fbxo32
Trim63
Ubiquitin ligase complex
Ubxn1
Proteasome
Protein degradation
Mstn
Acvr2b
Acvr1b
+p
Smad2
Smad3
Smad7
ATF4 target gene
Myh4
Atf3
Ppp1r15a
Eif4ebp1
Atf4
Mknk2
Eif4e
Protein synthesis
Stress granule
Spliceosome
Ribosome
Ddit4
mTORC1
Mtor
Akt1s1
Rps6kb1
Sesn1
AKT
Insr
Igf1r
Irs1
Pik3r3
Akt1
p-AKT
FOXO
Foxo1
FOXO1
Foxo3
Sgk1
Crebbp
Autophagy
Depp1
Rab7
Lysosome
Ctsd
Map1lc3a
Fusion with lysosome
Degradation of the innervisicle
Smcr8
Sqstm1
Pink1
Ulk1
Rb1cc1
Atg13
Atg101
ULK complex
Apoptosis
Ctsd
Xiap
Tnfsf10
Tnfrsf10b
Fadd
Casp8
Casp10
Casp7
Apoptosis
Gadd45g
Klf2
Klf4
Differentiation
Ppp1ca
Mylpf
Hey1
MyoD
Cdh15
Rock1
Daam1
Rhoa
Rock2
Wnt11
Fzd6
Dvl1
Rac2
Pak1
Mylk
Porcn
Rxra
Vav1
Myh7b
Increased DEG
Decreased DEG
Unchanged gene levels
Decreased protein
P-value = 0.072

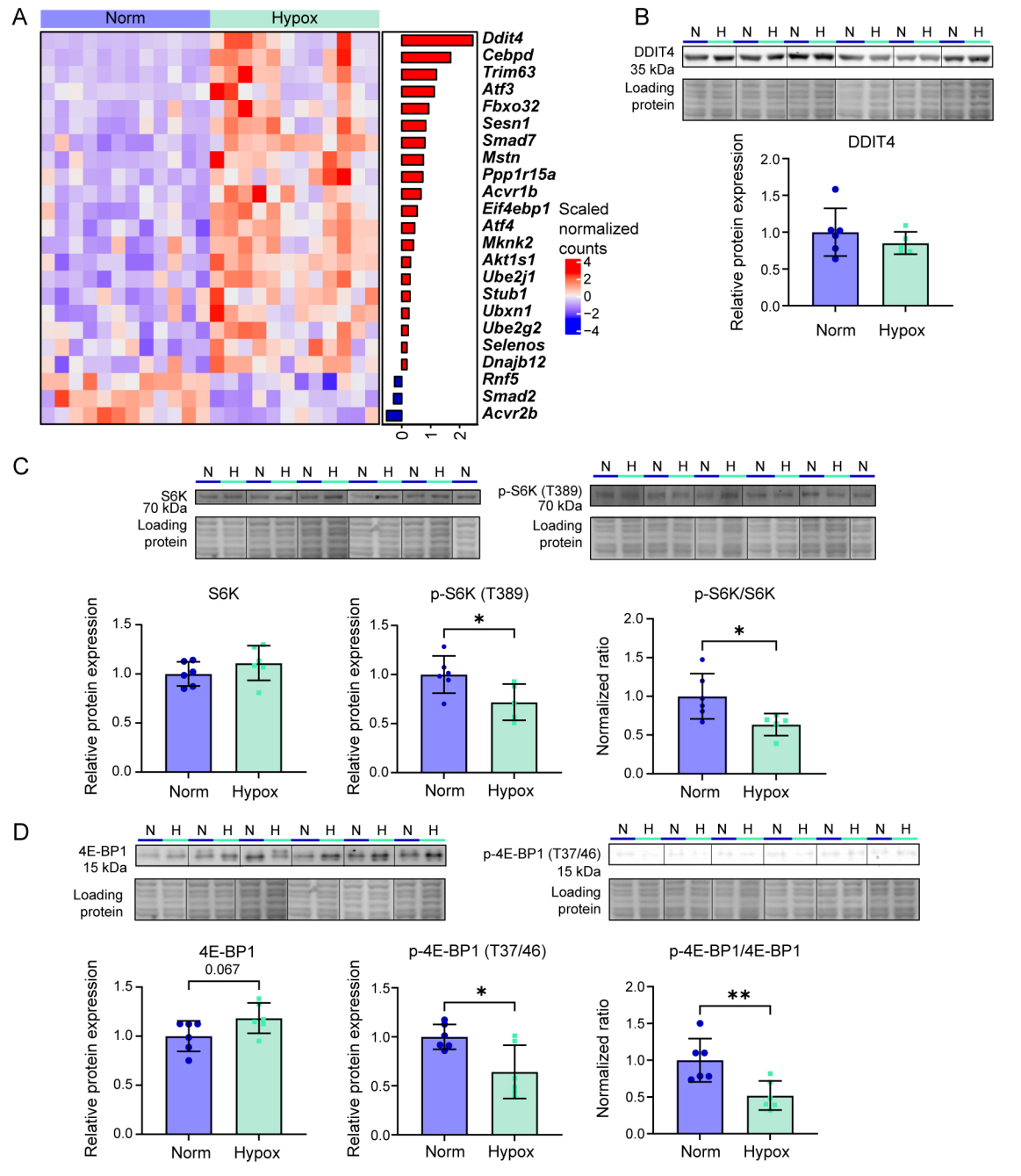
A
Norm
Hypox
Ddit4
Cebpd
Trim63
Atf3
Fbxo32
Sesn1
Smad7
Mstn
Ppp1r15a
Acvr1b
Eif4ebp1
Atf4
Mknk2
Akt1s1
Ube2j1
Stub1
Ubxn1
Ube2g2
Selenos
Dnajb12
Rnf5
Smad2
Acvr2b
Scaled normalized counts
4
2
0
−2
−4
0
1
2
B
N H N H N H N H N H N H
DDIT4
35 kDa
Loading protein
DDIT4
Relative protein expression
2.0
1.5
1.0
0.5
0.0
Norm
Hypox
C
N H N H N H N H N H N
S6K
70 kDa
Loading protein
p-S6K (T389)
70 kDa
Loading protein
S6K
Relative protein expression
1.5
1.0
0.5
0.0
Norm
Hypox
p-S6K (T389)
*
p-S6K/S6K
Normalized ratio
2.0
D
N H N H N H N H N H N H
4E-BP1
15 kDa
Loading protein
p-4E-BP1 (T37/46)
15 kDa
Loading protein
4E-BP1
0.067
p-4E-BP1 (T37/46)
p-4E-BP1/4E-BP1
**

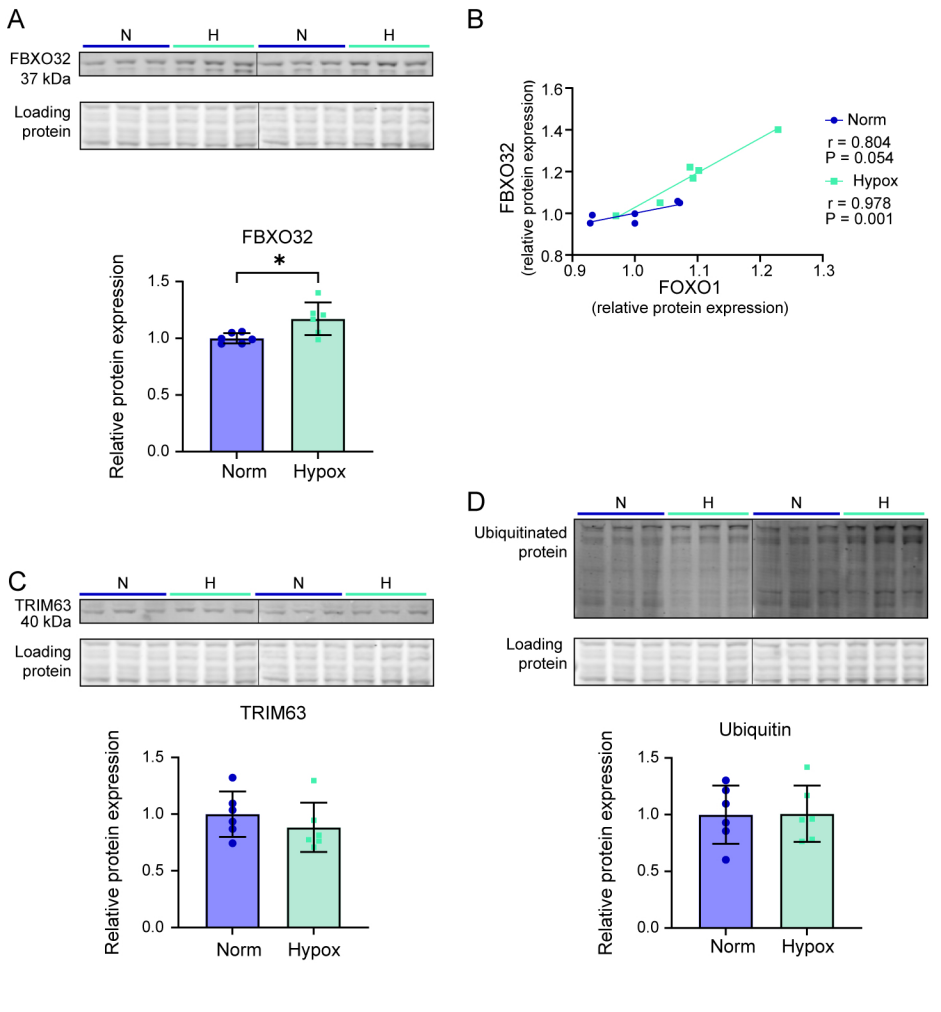
A
N
H
N
H
FBXO32
37 kDa
Loading
protein
FBXO32
Relative protein expression
1.5
1.0
0.5
0.0
*
Norm
Hypox
B
FBXO32
(relative protein expression)
1.6
1.4
1.2
1.0
0.8
0.9
1.0
1.1
1.2
1.3
FOXO1
(relative protein expression)
Norm
r = 0.804
P = 0.054
Hypox
r = 0.978
P = 0.001
C
N
H
N
H
TRIM63
40 kDa
Loading
protein
TRIM63
Relative protein expression
1.5
1.0
0.5
0.0
Norm
Hypox
D
N
H
N
H
Ubiquitinated
protein
Loading
protein
Ubiquitin
Relative protein expression
1.5
1.0
0.5
0.0
Norm
Hypox

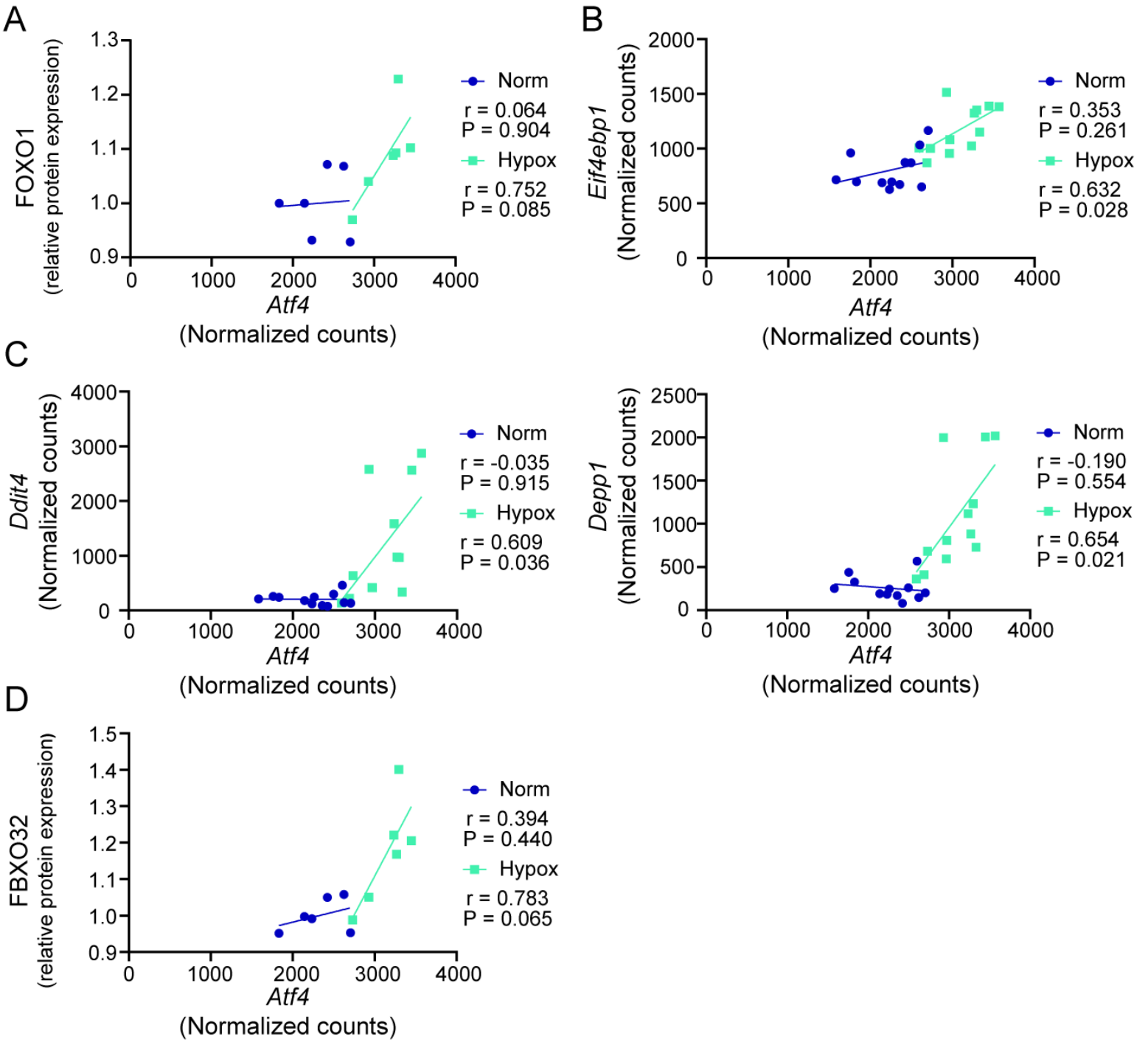
A
FOXO1
(relative protein expression)
1.3
1.2
1.1
1.0
0.9
0
1000
2000
3000
4000
Atf4
(Normalized counts)
Norm
r = 0.064
P = 0.904
Hypox
r = 0.752
P = 0.085
B
Eif4ebp1
(Normalized counts)
2000
1500
1000
500
0
Norm
r = 0.353
P = 0.261
Hypox
r = 0.632
P = 0.028
C
Ddit4
(Normalized counts)
4000
3000
2000
1000
0
Norm
r = -0.035
P = 0.915
Hypox
r = 0.609
P = 0.036
Depp1
(Normalized counts)
2500
2000
1500
1000
500
0
Norm
r = -0.190
P = 0.554
Hypox
r = 0.654
P = 0.021
D
FBXO32
(relative protein expression)
1.5
1.4
1.3
1.2
1.1
1.0
0.9
Norm
r = 0.394
P = 0.440
Hypox
r = 0.783
P = 0.065

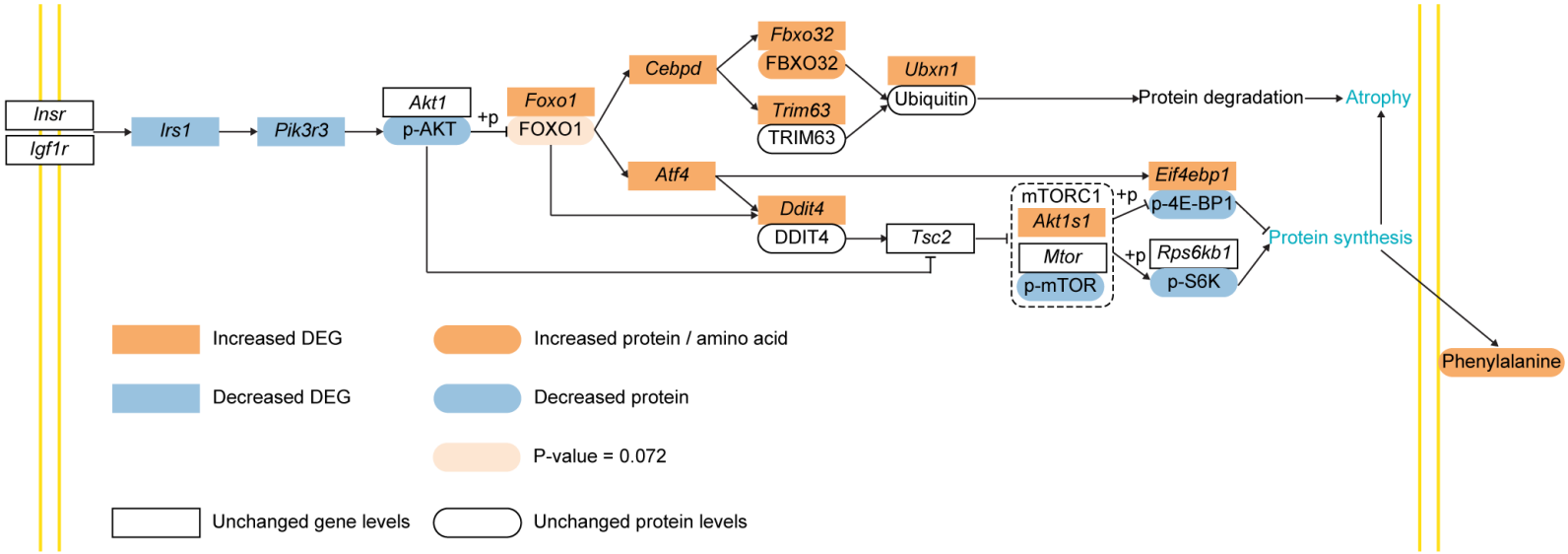
Insr
Igf1r
Irs1
Pik3r3
Akt1
p-AKT
+p
Foxo1
FOXO1
Cebpd
Fbxo32
FBXO32
Trim63
TRIM63
Ubxn1
Ubiquitin
Protein degradation
Atrophy
Atf4
Eif4ebp1
p-4E-BP1
Ddit4
DDIT4
Tsc2
mTORC1
Akt1s1
Mtor
p-mTOR
+p
Rps6kb1
p-S6K
Protein synthesis
Phenylalanine
Increased DEG
Decreased DEG
Unchanged gene levels
Increased protein / amino acid
Decreased protein
P-value = 0.072
Unchanged protein levels

Acute Hypoxic Response on Proteostasis of Skeletal Muscle in Prepubertal Mice

METHODS

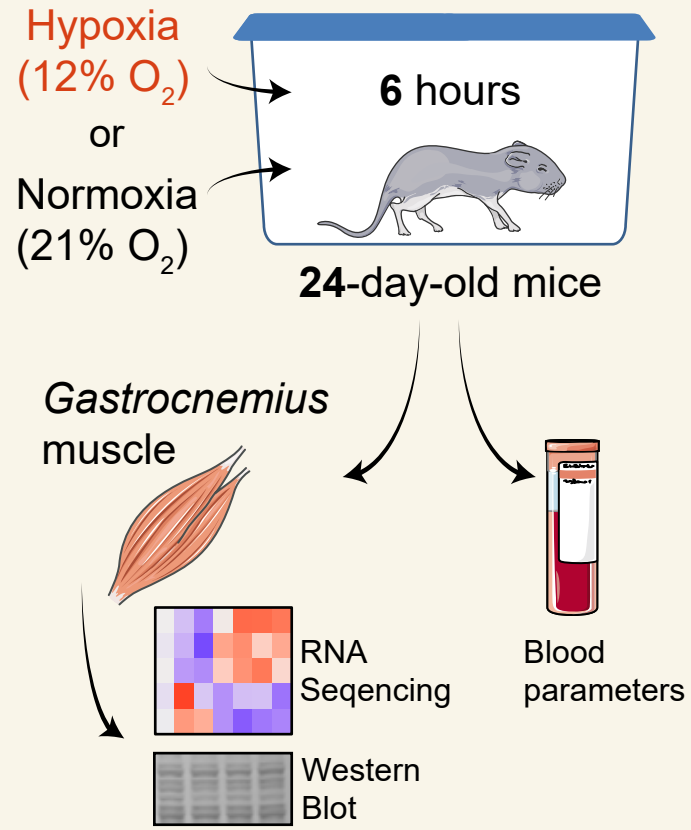

OUTCOMES

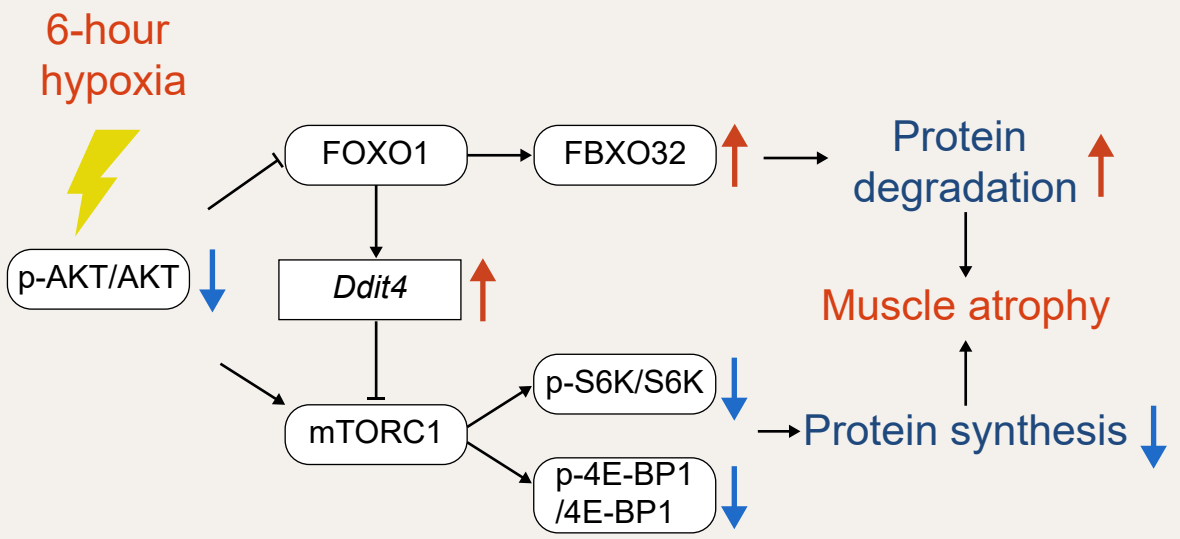

CONCLUSION

Acute hypoxia activates protein degradation (FOXO1) and inhibits protein synthesis (mTORC1) in growing *M. gastrocnemius.*